Geomorphology 139–140 (2012) 495–505

Contents lists available at SciVerse ScienceDirect

Geomorphology

journal homepage: www.elsevier.com/locate/geomorph

# Cirque overdeepening and their relationship to morphometry

Marek Křížek *, Klára Točadlová, Zbyněk Engel

Department of Physical Geography and Geoecology, Faculty of Science, Charles University in Prague, Albertov 6, 128 43 Praha 2, Czech Republic

ARTICLE INFO

*Article history:*
Received 25 February 2011
Received in revised form 18 November 2011
Accepted 19 November 2011
Available online 1 December 2011

*Keywords:*
Cirque morphometry
Overdeepening
*k*-curve
Bohemian Massif (the Czech Republic, Germany, Poland)

ABSTRACT

Shape and size characteristics of cirques and their changes and mutual relationships include not only spatial and descriptive aspects but also genetic attributes. The goals of this article were to define an application of *k-curve* (sensu Haynes, 1968) that describes the extent of cirque overdeepening and to identify *k*-curve equation input variables. The *k*-values depend on the profile location, and hence, a clear definition of the cirque profile position is necessary. Therefore, ideal profiles were delineated through the steepest part of the cirque headwall (*k*-steepest, $k_s$) or through a point on the cirque crest that had a maximal elevation (*k*-highest, $k_h$). Knowledge of the cirque headwall height allows for the mathematical (theoretical) calculation of cirque overdeepening (i.e., the maximum depth of the cirque floor, sedimentary filling of the cirque floor). Further, the goal of this study was to analyse and compare cirque classification methods according to the extent of overdeepening and standard morphometric characteristics. As a training data set, 27 example cirques of the Bohemian Massif (Giant Mts., Šumava Mts., and Hrubý Jeseník Mts.) and a total of 12 morphometric characteristics were used in the analyses. Cirques were classified into two groups using cluster analysis based on the extent of overdeepening (*k*-values: $k_h$ and $k_s$). A mutual relationship between cluster analysis classifications and classifications based on morphometric characteristics (*L*/*W*, *H*, and *3D*/*2D*) was determined using general discriminant analysis. The classification of cirques based on other characteristics corresponded closely (in total, 81% for the first group and the cross-validation group) with cirque classifications based on the degree of overdeepening (*k*-value).



## 1. Introduction

In many published studies, cirques have been defined and characterised using a range of morphometric characteristics (Graf, 1976; Evans, 1977; Vilborg, 1977; Aniya and Welch, 1981; Evans and Cox, 1995; Haynes, 1998; Davis, 1999; García-Ruiz et al., 2000; Federici and Spagnolo, 2004; Brook et al., 2006; Ruiz-Fernández et al., 2009). In addition to the analysis of morphometric characteristics and evaluations of their mutual dependences, these studies also described the relationships between the size and shape characteristics of cirques and exposure, geological conditions, and the location of snow sources. The aim of this article is not to study all relationships mentioned above, but to focus on determination of the degree of cirque overdeepening using *k-curve* (Haynes, 1968) and its comparison with cirque morphometry. From a mathematical point of view, this article analyses the quantities (variables) that enter into the *k*-curve and its subsequent application in real relief; although *k*-curve has been mentioned in some published studies, it has not been satisfactorily explained and its essence has not been described (Vilborg, 1977; Martini et al., 2001; Rasemann et al., 2004; Brook et al., 2006; Bennett and Glasser, 2009; Benn and Evans, 2010). A correct definition of *k*-curve as a part of glacial erosion landform analyses can contribute to the identification of the development and intensity of mountain glaciation. Gordon (1977, p. 192) said that "if it is valid to assume a space–time transformation that cirque development is a function of cirque size, then the relationships between the cirque size and shape variables have important implication for the mode of cirque development."

Another question is how cirque classification based on *k*-values differs from cirque classification based on commonly used morphometric characteristics. Cirques can be divided into categories according to their *k*-values and this classification can be combined with classifications based on typical morphometric characteristics. In other words, a chosen group of cirques can be categorised based on the morphologic features (morphologic indices, sensu Evans and Cox, 1995) and a genetic perspective (*k*-curve, sensu Haynes, 1968).

The main goals of this article are to define the use of *k*-curve as a descriptive index that characterises cirque overdeepening and to analyse and compare the classification of cirques according to the degree of overdeepening (*k*-curve) and standard morphometric characteristics based on cirques in the Bohemian Massif. The task of this paper is to determine whether the *k*-curve brings some new information on the morphology of cirques, or whether it can be expressed in other established morphometric characteristics.

Comparison of overdeepening (*k*-values) and morphometric characteristics was performed on 27 cirques in the Bohemian Massif. These cirques form a homogeneous group, with similar development

* Corresponding author. Tel.: +420 22 19 95 523; fax: +420 221 951 367.
*E-mail addresses:* krizekma@natur.cuni.cz (M. Křížek), vocadlov@natur.cuni.cz (K. Točadlová), engel@natur.cuni.cz (Z. Engel).

0169-555X/$ – see front matter © 2011 Elsevier B.V. All rights reserved.
doi:10.1016/j.geomorph.2011.11.014

and shape of relief, the same character and age of glaciation, with similar paleoclimatic conditions and similar postglacial development.

## 2. Regional setting

During Pleistocene cold periods, the Bohemian Massif was located in a periglacial zone in a foreland region of continental glaciation (Czudek, 2005), and mountain glaciation occurred only in the northern (the High Sudetes) and southern (the Šumava Mts.) fringes of the Bohemian Massif. Small cirque glaciers, with tongues up to a few kilometres long, altered the relief and formed the cirques that are currently one of the dominant characteristic landforms of the local landscape. The relief of glacial landforms in the Bohemian Massif was defined and described as early as the nineteenth century (e.g., Bayberger, 1886; Partsch, 1894). These reports were followed by other studies on the glacial modification of the High Sudetes (e.g., Vitásek, 1924; Prosová and Sekyra, 1961; Chmal and Traczyk, 1999; Migoń, 1999; Mercier et al., 2000; Engel, 2007; Engel et al., 2010) and the Šumava Mts. (Rathsburg, 1928; Priehäusser, 1930; Kunský, 1948; Ergenzinger, 1967; Votýpka, 1979; Hauner, 1980; Raab and Völkel, 2003; Vočadlová et al., 2007; Vočadlová and Křížek, 2009; Mentlík et al., 2010); however complex comparative studies have not been carried out.

The Bohemian Massif is a Hercynian geological unit (Chlupáč et al., 2002) and includes the majority of the Czech Republic and parts of the frontier regions of Germany, Poland, and Austria (Fig. 1). The High Sudetes and the Šumava Mts. are fault-block ranges with summit plateaus and this terrain had an important role in the origin of the Late Pleistocene mountain glaciation. Snow that was blown from summit plateaus by prevailing westerly winds (Meyer and Kottmeier, 1989; Isarin et al., 1997) onto leeward preglacial valley heads helped to create cirque and valley glaciers with tongues that are only a few hundred metres to a few kilometres long (Jeník, 1961). Deglaciation of the Bohemian Massif occurred at the end of the Late Pleistocene.

The Šumava Mts. (called the Bavarian Forest on the German side and the Bohemian Forest on the Czech side of the state border, Fig. 1) are mainly composed of metamorphic rocks (gneisses, mica schists, phyllites, granulites, and migmatites) permeated by younger igneous rocks (granites, tonalities, and granodiorites) (Babůrek et al., 2006). The highest peak is Grosser Arber (1456 m asl). In the mountain range, eight of 13 cirques are filled with lakes: Černé jezero, Čertovo jezero, Laka, Prášilské jezero (compound cirque), Plešné jezero, Kleiner Arbersee, Grosser Arbersee, and Rachelsee. The predominant view is that a smaller extent of glacier covers (cirque or short valley glaciers) was present here in times of maximal glaciation (Hauner, 1980; Raab, 1999; Reuther, 2007). Evidence of the Late Pleistocene glaciation (MIS 2) in the Šumava Mts. has been found, although no convincing evidence for older glaciation has been existed (Bayberger, 1886; Rathsburg, 1928; Priehäusser, 1930; Ergenzinger, 1967; Hauner, 1980). The Pleistocene snow equilibrium line altitude (according to the maximum elevation of lateral moraines method, MELM) corresponding to the last glaciation was found between 925

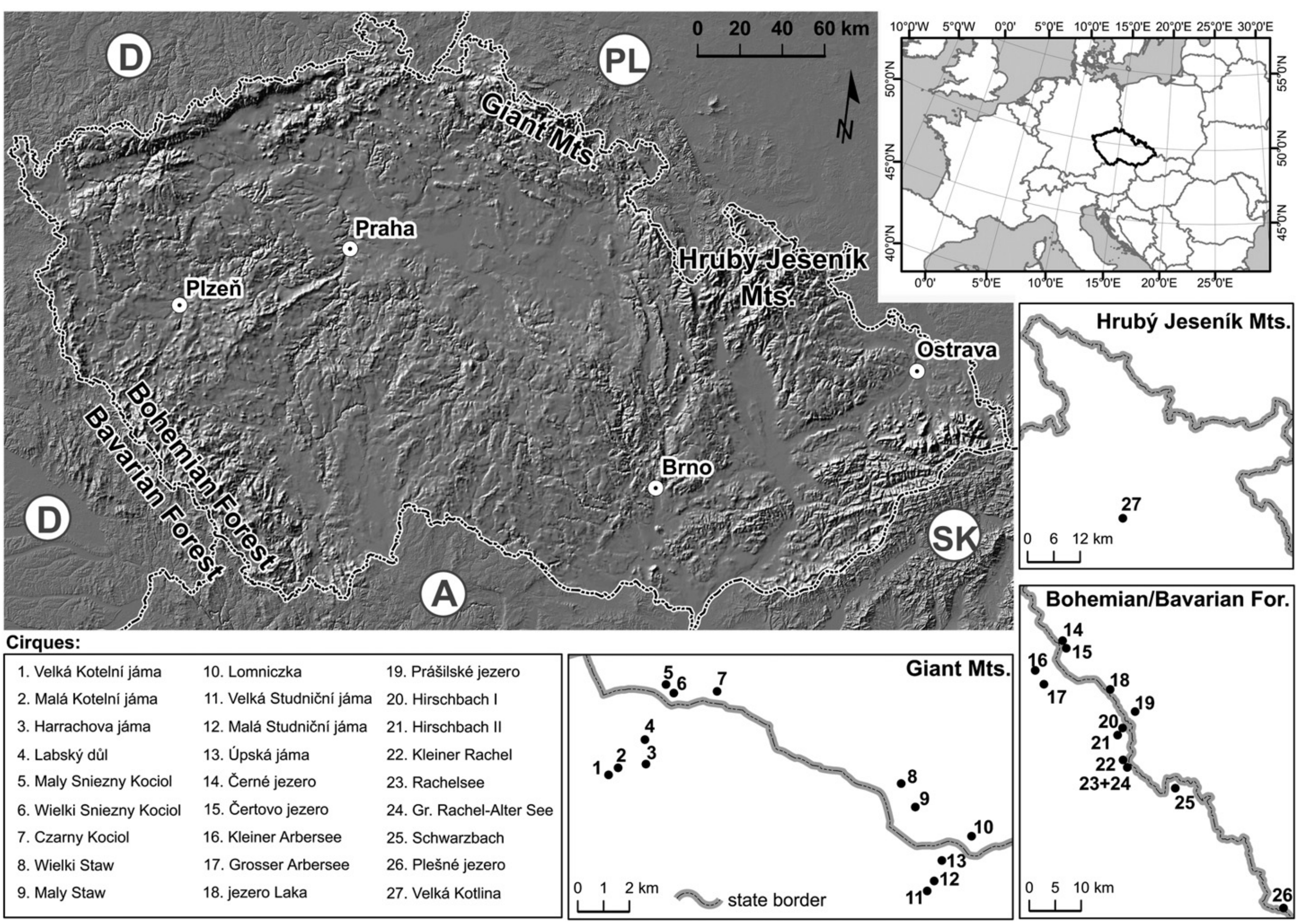


**Fig. 1.** Distribution of cirques in the Bohemian Massif.

and 1115 m asl (Hauner, 1980; Raab, 1999; Vočadlová and Křížek, 2005; Mentlík et al., 2010). Recent research in the Šumava Mts. has shown that the cirque floors were free of ice prior to ~14,500–14,000 cal YBP (Raab and Völkel, 2003; Reuther, 2007; Mentlík et al., 2010)

The Giant Mts. (called Krkonoše on the Czech side and Karkonosze on the Polish side of the state borders) represent the western part of the High Sudetes and mainly consist of Proterozoic and Paleozoic methamorphites (gneiss, mica schist, phyllite, and quartzite) and plutonic rocks (granite) can be found (Chlupáč et al., 2002). This mountain range on the Czech and Polish border has fault-generated mountain fronts on the southern and northern side, extended summit plateaus (area up to a few square kilometres). Mt. Sněžka (1602 m asl) is the highest peak. The front of the Scandinavian ice sheet approached immediately the northern foreground of the Giant Mts. during the Early Saalian (MIS8, 440–430 ka BP) (Hall and Migoń, 2010). More morphologic evidence of glacial alteration has been obtained from the Giant Mts. than from all other studied ranges of the Bohemian Massif. A total of 13 cirques (six on the Polish side, seven on the Czech side) have been described in this region. Tongues of the largest glaciers on the Czech side of the Giant Mts. (glacier of Labský důl valley and Obří důl valley) reached a maximum of up to 5 km in length (Králík and Sekyra, 1969). An equilibrium snow line altitude occurred at 1060–1170 m asl during the oldest glacier oscillation at the end of the Pleistocene. Glacial accumulation landforms from the last Würm glaciation were preserved on the Czech side, whereas relicts also of Riss moraines were found on the Polish side (Traczyk, 1989; Chmal and Traczyk, 1999). Recent research has shown that the last phase of deglaciation occurred prior to ~11,000 cal YBP (Engel et al., 2010).

The Hrubý Jeseník Mts. form the eastern part of the High Sudetes and are mainly composed of metamorphic rocks (gneiss, mica schist, phyllite, quartzite, and erlan) (Chlupáč et al., 2002). The main ridge of the Hrubý Jeseník Mts. that includes summit plateaus (1300–1450 m asl) has a north–south orientation. Mount Praděd (1492 m asl) is the highest peak. Today, this mountain range has the lowest rate of glacial modification because of constrains imposed by preglacial relief

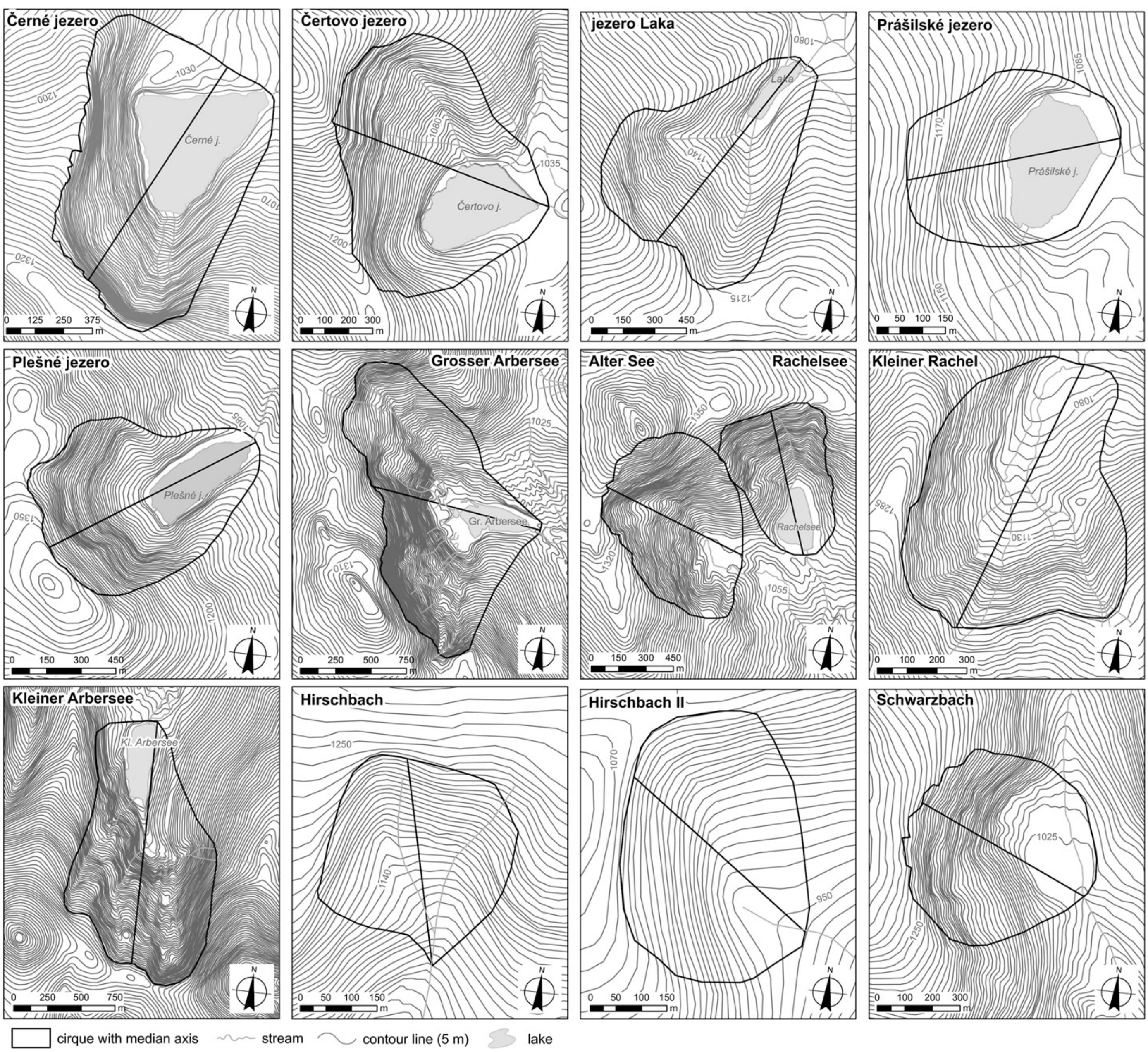


Fig. 2. Cirques of the Šumava Mts. with marked median axis.

(Migoń, 1999) and the low resistance of rocks which contributed to rapid weathering and big rate of postglacial modification of the relief. Only one cirque, Velká kotlina, can be found in the valley head of the Moravice River (Prosová, 1958; Czudek, 2005). This cirque has an east–southeast position relative to the main ridge of the Hrubý Jeseník Mts. and is situated below its largest summit plateau, which supplied the glacier with snow. This glacier was 600 m in length (Prosová, 1958), and its terminal moraine is situated at 1060 m asl The snowline altitude of the glacier during the last glaciation was defined by Vitásek (1924) to be 1150 m asl, which approximately corresponds with the altitude of the cirque floor.

## 3. Methodological approach

### 3.1. Morphometric (planimetric and hypsometric) characteristics of cirques

Calculations associated with the determination of planimetric and hypsometric indices that describe cirques were used for morphometric analyses. The most frequently used indices that define the size and shape of cirques were chosen. Data used for morphometric analyses were acquired from published geomorphologic studies, from aerial photos, from a digital elevation model (DEM), and from field mapping. A DEM of 3 × 3 m pixel size was created from the contour data of military topographic maps DMÚ 25 at a scale of 1:25,000 with a 5-m contour interval and a basic positional accuracy of up to 10 m. Cirque borders were delineated according to the crest limit and threshold and by the moraine crest line if the moraine covered the threshold. Step-like cirques were considered as one unit where the lowest-lying cirque was included to analyse landforms corresponding to maximal extent of glaciation in a particular locality (Kleiner Arbersee, Grosser Arbersee, Grosser Rachel-Altersee, and Prášilské jezero). A total of 27 cirques were analysed (five cirques on the Czech side of the Šumava Mts., eight cirques on the German side of the Šumava Mts., seven cirques on the Czech side of the Giant Mts., six cirques on the Polish side of the Giant Mts., and one cirque in the Hrubý Jeseník Mts.) (Figs. 2 and 3).

The following features that describe the cirque size were used in the morphometric analysis: height ($H$), length ($L$), width ($W$), plan

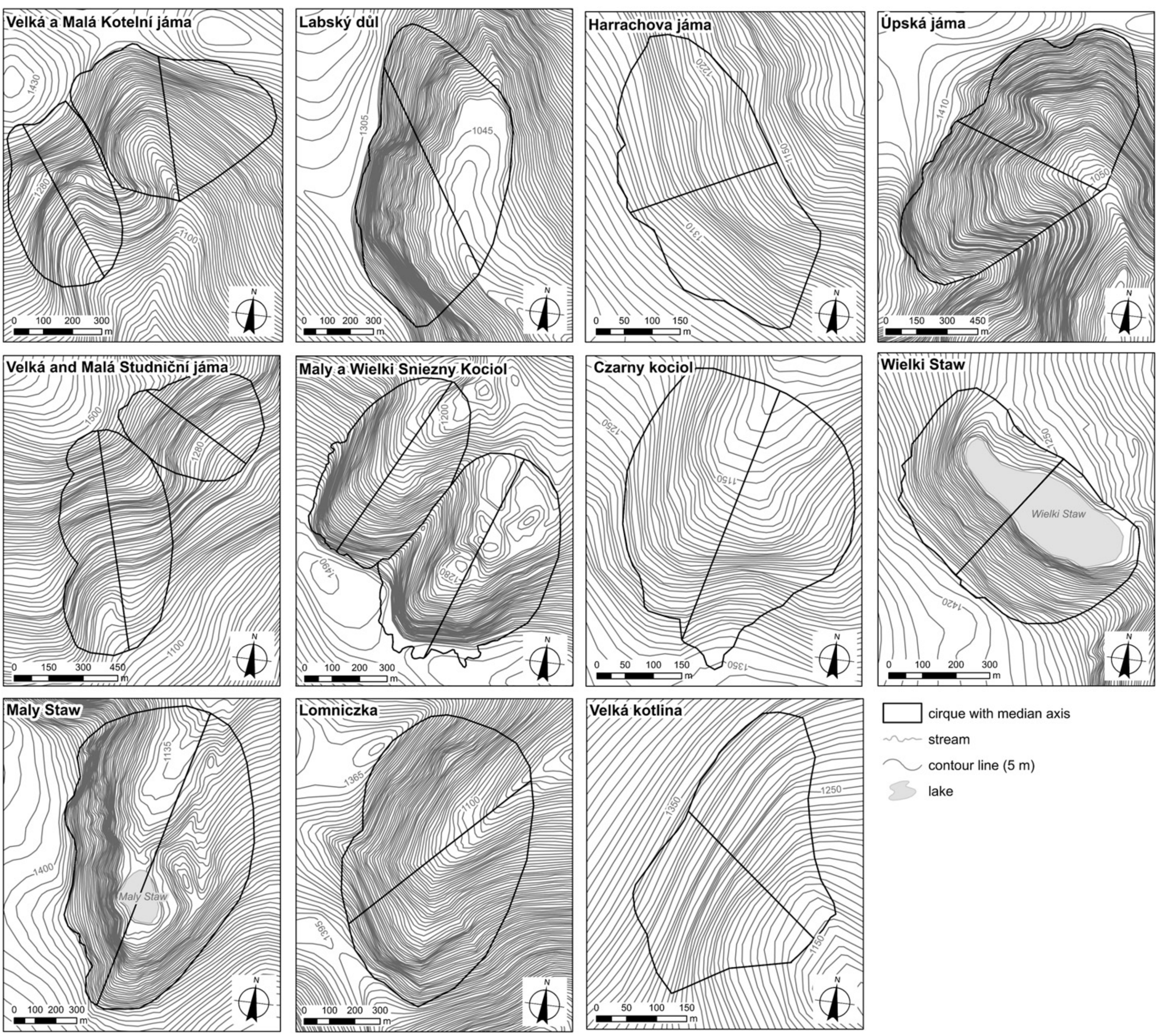


Fig. 3. Cirques of the High Sudetes with marked median axis.

area (*2D*, area of the planar projection of the relief), volume (*V*), mean slope, aspect of the cirque median axis, and surface area (*3D*, area of the real relief). Based on these measurements, indices that describe the shape of cirques were calculated: cirque length to height ratio (*L/H*), cirque length to width ratio (*L/W*), width to height ratio (*W/H*), and the surface area to plan area ratio (*3D/2D*).

The cirque height (*H*) represented the difference between the lowest and the highest altitude within a cirque (sensu Aniya and Welch, 1981; García-Ruiz et al., 2000; Federici and Spagnolo, 2004). Similar to other studies (Evans and Cox, 1995; Federici and Spagnolo, 2004), cirque length (*L*) was measured along the median axis — a line drawn from the cirque focus (middle of cirque threshold) to the crest — such that the area on the left was equal to the area on the right. The (maximum) width (*W*) was measured at a right angle to the median axis. Altitudes ($E_{min.}$, $E_{max.}$, and $E_{mean}$), cirque areas (*2D* and *3D*), and the mean gradient were derived from the DEM by using GIS tools. Cirque volume (*V*) was calculated as $V = 0.5(H \times L \times W)$ (Gordon, 1977; Davis, 1999). The cirque aspects were defined as the median axis aspect and were classified into eight categories: N, NE, E, SE, S, SW, W, and NW. The DEM was used to derive the cirque plan areas (*2D*) based on the area of the orthographic floor projection of the cirque. The cirque surface areas (*3D*) were derived from the DEM and represented the actual area of a cirque surface. The *3D/2D* ratio reflected an area-relative elevation relationship (vertical relief segmentation; relative relief) of a cirque. The *L/H* ratio (gradient) illustrated the cross-sectional shape of the cirque, *L/W* ratio described the planimetric shape (indicated circularity or cirque elongation), and the *W/H* ratio indicated the extent of cirque incision (Graf, 1976; García-Ruiz et al., 2000).

### 3.2. Construction, characteristics and application of k-curve

Cirque overdeepening is defined by a *k*-coefficient based on the equation

$$y = k(1-x)e^{-x} \tag{1}$$

which is called the *k*-curve (Haynes, 1968) (Fig. 4). To calculate a *k*-curve, a longitudinal section of a cirque was constructed, and the horizontal (*a*) and vertical (β) distances between the headwall crest and headwall foot were determined. These data were used for the calculation of *k*-coefficients. Headwall foot positions were determined based on the shape of the longitudinal section curve. Two *k*-coefficients were calculated for each cirque depending on the location of the longitudinal profile. The first *k*-coefficient (*k*-steepest, $k_s$) was calculated based on the profile crossing the steepest part of the cirque headwall, and the second *k*-coefficient (*k*-highest, $k_h$) was calculated based on the profile running down from a point on the cirque

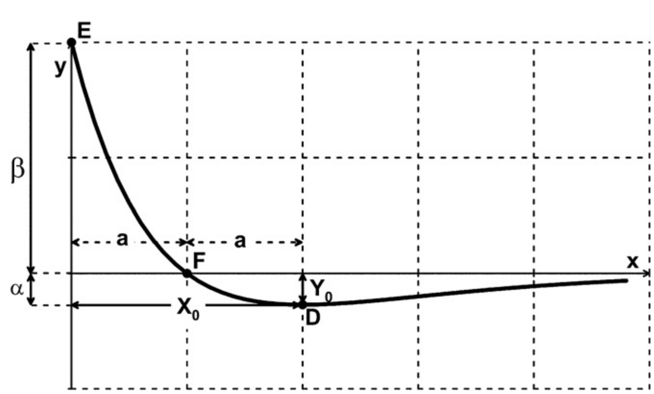


**Fig. 4.** Graph of the *k*-curve for $k = 2$. Input variables that are used for the calculation of *k*-curves are marked. E — cirque crest, F — headwall foot, and D — deepest point of the cirque floor.

crest with a maximal altitude across the cirque floor. Lines of both profiles went perpendicularly through the contours and passed as closely as possible through the lowest part of the cirque floor.

The domain of definition of Eq. (1) was $(-\infty,+\infty)$; however, with respect to *x*, which described the lengths, we accepted that the domain of this function was $(0,+\infty)$. Other characteristics of the *k*-curve resulted from the first (Eq. (2)) and second derivatives (Eq. (3)) of the *k*-curve function (Eq. (1)); i.e.

$$y' = -ke^{-x}(2-x) \tag{2}$$

$$y'' = ke^{-x}(3-x). \tag{3}$$

For the first derivative, $y' = 0$ when $x = 2$; the second derivative at point $x = 2$ was nonzero. Therefore, it followed that the function Eq. (1) had a local extreme at point $x = 2$. The first derivative Eq. (2) showed that $y' < 0$ within the interval (0,2) and $y' > 0$ in the interval $(2,\infty)$. The *k*-curve function (Eq. (1)) reached a local minimum at the point $x = 2$. Therefore, the *k*-curve ran through the deepest point of the cirque. Thus, the *k*-value could be defined based on the difference in altitude between the lowest point of the cirque and the foot of cirque headwall (Fig. 4) because values $X_0$ (horizontal distance between the deepest point of the cirque and the cirque crest) and $Y_0$ (difference in elevation between the deepest point of the cirque and the foot of the cirque headwall) could be determined by geomorphologic mapping. However, it is necessary to transform the real values $X_0$ and $Y_0$ (presented in metres or kilometres) into *k*-curve metrics and make computations using these transformed values. In other words, for the deepest point of the cirque $(x = 2)$, $k = -ye^2$ where the *y* value was defined as $y = 2Y_0/X_0$, whereas the value $Y_0$ had a negative sign with respect to the defined coordinate system (see Fig. 4).

Another important characteristics resulting from the *k*-curve function (Eq. (1)) was the relationship between the cirque floor deepening (α; cirque floor deepening means an elevation difference between the headwall foot and the cirque floor) and the height of the cirque headwall (β; cirque headwall height means an elevation difference between the headwall foot and the headwall crest) that was constant and corresponded to $\alpha/\beta = -e^{-2}$. When calculating β, $x = 0$ for the cirque crest, and consequently, $y = k(1–0)e^{-0}$ and $y = k$; when calculating α with $x = 2$, $y = k(1–2)e^{-2}$, and $y = -ke^{-2}$. A constant α/β ratio was used as a mathematical approximation of the cirque floor deepening based on knowledge of the cirque headwall height, which was multiplied by $-e^{-2}$. This procedure was used in cases where the cirque floor was covered by sediments of unknown thickness or by a lake of unknown depth.

Based on the definition and character of the *k*-curves, evident is that *k*-coefficient could never be negative because $\beta = k$ and $\alpha = -ke^{-2}$. Otherwise, the basic presumption that a cirque crest was situated higher than the foot of the cirque headwall of the appropriate cirque would not be valid.

### 3.3. Statistical evaluation

All statistical operations were performed using the programme STATISTICA (StatSoft, Inc., 2009). The studied cirques were divided into groups based on cluster analysis (tree clustering), with the appropriate values of $k_h$ and $k_s$ as the input variables of correlation morphometric characteristics were expressed as Pearson correlation coefficients, with the significance of differences in single characteristics was tested using t-tests with a confidence level of $p = 0.05$.

General discriminant analysis (GDA) was executed for a select subset of all studied morphometric characteristics (basis). The basis of the morphometric characteristics was explicitly defined as the largest set of independent morphometric characteristics (i.e., those characteristics that were not mutually correlated). The choice of basis members was made as follows: primarily, a characteristic with the smallest number of significant correlations with other morphometric characteristics was found. This characteristic was the first member of the basis. Other members of the basis were defined in the same manner from the set of remaining morphometric characteristics. The basis of morphometric characteristics (in accordance with the above described procedure) consisted of *L/W*, *H*, and *3D/2D*. The observed cirque classifications were determined based on the classification of cirques into groups according to the cluster analysis described above. The GDA classification predictors were *L/W*, *H*, and *3D/2D*. Classification accuracy was defined using a cross-validation method (Huberty, 1994) that assessed the predictive accuracy of a model in a test sample (sensu STATISTICA; StatSoft, Inc., 2009). Out of a set of 27 cirques, 14 were randomly selected by random number generation. Standardised canonical discriminant function coefficients λ (sensu Manly, 2005) were defined for this selected group of cirques (first group of analysis) using STATISTICA (StatSoft, Inc., 2009): $\lambda(H) = 0.06413$, $\lambda(L/W) = -0.82299$ and $\lambda(3D/2D) = -1.00393$. These same derived coefficients were also used for the second part of the set in accordance with the cross-validation method. Classification matrices were created for both subsets using STATISTICA (StatSoft, Inc., 2009) (sensu Meloun et al., 2005). The matrices represented the classification accuracy when using the same discriminant function coefficients; the inclusion of single cirques within a given class was formulated based on posterior probability according to the same procedure used for the classification matrices.

## 4. Results

### 4.1. Cirque morphometry

The cirques in the Bohemian Massif were located in leeward areas; i.e. they faced northeast (seven cirques), southeast (seven cirques), or to the east (four cirques) (Table 1). Aspect differences between single mountain ranges were very small.

The following characteristics of cirques were defined: cirque size features (height (*H*), length (*L*), width (*W*), area (*2D*), volume (*V*), mean inclination, and surface area) and shape features (ratio of length to height (*L/H*) and ratio of length to width (*L/W*), ratio of width to height (*W/H*), ratio of surface area to *2D* area (*3D/2D*), and a *k*-coefficient).

The majority of the cirques (75%) had *H* values within the range of 116 to 324 m (Table 1). The average height of cirque headwalls (*H*) was greatest in the Czech part of the Giant Mts. (310 m). Average cirque headwall heights in the other localities were between 255 and 269 m. Three quarters of the cirques were between 278 and 975 m long and 360 and 826 m wide. Average cirque lengths were highest in the Bohemian Forest (915 m) and were shortest for cirques in the Czech part of the Giant Mts. (608 m). The cirques in the Giant Mts. were relatively wide compared to cirques in the Šumava Mts. (788 vs. 620 m, respectively). On average, the cirques in the Šumava Mts. had distinctively larger areas than the cirques in the Giant Mts. (62 vs. 38 ha, respectively). South- and southeast-oriented cirques showed lower average values of all size characteristics (*H*, *L*, *W*, *2D*, and *V*), with the exception of inclination values that were slightly higher (27.4°). In contrast, the largest cirques were oriented towards the east. These eastward-oriented cirques also had the smallest mean gradient (23.8°), and they were only surpassed in length by cirques oriented to the north. Cirques oriented to the north were shallower, longer, and narrower. Cirques oriented to the east were wider and shorter. Cirques oriented to the south were deeper and more closed.

The *L/H* ratio varied between 1.5 and 5.3, and 75% of the cirques had *L/H* values of up to 3.68. The cirques in the Bohemian Massif were shallower than cirques of the Giant Mts. with lengths that exceeded their height. Three-quarters of the cirques had *L/W* values that were less than 1.33. Only one quarter of the cirques had *W/H* ratios that exceeded 3.22.

The *3D/2D* ratios varied between 1.04 and 1.22 with an average value of 1.15. The Laka cirque had the smallest *2D/3D* value, and the Harrachova jáma cirque had the greatest *3D/2D* ratio.

The *k*-coefficient, which indicated the degree of cirque overdeepening, reached values of 0.35–1.00 for $k_h$ and 0.30–1.21 for $k_s$. Three-quarters of the cirques had $k_h$- and $k_s$-values that were $<0.77$ and 0.82, respectively (Table 1).

### 4.2. Cirque morphometric analysis and classification

A significant difference ($p$-value $= 0.05$) between overdeepening (*k*-values) of cirques in the Šumava Mts. and cirques in the High Sudetes was observed based on one-way ANOVA analyses ($k_h$: $F(1;25) = 12.161$; $p = 0.0018$, $k_s$: $F(1;25) = 10.329$; $p = 0.0036$); cirques in the Šumava Mts. had average $k_h$ and $k_s$ values of 0.56 and 0.63, respectively, and cirques in the High Sudetes had higher average $k_h$ and $k_s$ values of 0.74 and 0.84, respectively.

Correlation analyses (Table 2) showed that cirque length (*L*) is most often significantly correlated feature. As expected, the highest correlations were observed between surface area (*3D*), *2D* area, and cirque volume (*V*). The *3D/2D* ratio and mean cirque inclination had the greatest positive correlation. In contrast, the *L/W* ratio had the lowest number of significant correlations (Table 2).

The basis of morphometric characteristics, which was the largest set of morphometric characteristics not correlated with one another, was represented by the *L/W* ratio, *H*, and *3D/2D* ratio. The cirques were classified into groups according to the degree of overdeepening (i.e., $k_h$ and $k_s$ values). Two main cirque clusters (Fig. 5) that were joined at a linkage distance of ~43 were obtained. The cirques were classified into two groups (see Fig. 5 and Table 1) according to these clusters.

A joint classification based on the degree of cirque overdeepening expressed by coefficients $k_h$ and $k_s$ and morphometric characteristics (*H*, *L*, *W*, *L/H*, *L/W*, *V*, *2D* area, surface area (*3D*), *3D/2D*, and mean inclination), rather than their base (*L/W*, *H*, and *3D/2D*), was determined using discriminant analysis. The consistency of cirque classifications based on $k_h$ and $k_s$ was high when regarding the morphometric basis (Table 3): 93% accuracy for the first group of analyses, 69% for the cross-validation group, or 81% for both groups together. In the first group of analyses, for which discriminant functions were defined, the Grosser Arbersee cirque was classified to other class of cirques (Table 4). In the cross-validation, a group of four cirques (the Malá Kotelní jáma, Kleiner Arbersee, Wielki Staw, and Łomniczka cirques) was, from statistical point of view, incorrectly classified (these cirques were classified to other class).

## 5. Discussion

### 5.1. Problems associated with k-curve input data and optimisation of k-curve input data

Mathematical analyses of *k*-curve functions and the definition of the variables *x* and *y* illustrated several limitations in the application of *k*-curves to the morphometric description of cirques. The main problem associated with the *k*-curve application (see Section 3.2) was the appropriate determination of the headwall foot zone and the appropriate choice of longitudinal profile locations used in the calculation of *k*-coefficients. Evident was that the profile location determined the final *k*-value (Fig. 6). To ensure an unambiguous computational technique and comparability of results, one profile was routed through the steepest part of the cirque headwall, and the second profile went through the highest point of the cirque crest. Considering that a *k*-curve describes glacial erosion relief (sensu Haynes, 1968), the position of the headwall foot (point F, Fig. 6)

**Table 1**
Morphometric characteristics of the Bohemian Massif cirques.

| Cirque name | GPS position | $k_h$ | $k_s$ | $E_{max.}$ | $E_{min.}$ | $E_{mean}$ | $H$ (m) | $L$ (m) | $W$ (m) | $L/H$ | $L/W$ | $W/H$ | Volume ($10^6$ m$^3$) | 2D area (ha) | Surface area (ha) | 3D/2D | Mean gradient (°) | Median axis aspect | Lithology[a] |
|---|---|---|---|---|---|---|---|---|---|---|---|---|---|---|---|---|---|---|---|
| Černé jezero | 49° 10′ 46″ N, 13° 10′ 57″ E | 0.74 | 0.76 | 1321 | 968 | 1084 | 353 | 1111 | 887 | 3.15 | 1.25 | 2.52 | 173.74 | 86.32 | 100.09 | 1.16 | 25 | NE | MS |
| Čertovo jezero | 49° 09′ 54″ N, 13° 11′ 48″ E | 0.54 | 0.60 | 1315 | 992 | 1116 | 323 | 901 | 1100 | 2.79 | 0.82 | 3.40 | 160.21 | 71.42 | 78.57 | 1.10 | 23 | E | MS, PG |
| Laka | 49° 06′ 37″ N, 13° 19′ 40″ E | 0.39 | 0.39 | 1304 | 1081 | 1157 | 223 | 1080 | 803 | 4.84 | 1.34 | 3.60 | 96.70 | 68.92 | 71.93 | 1.04 | 15 | NE | PG, GD |
| Prášilské jezero[b] | 49° 04′ 31″ N, 13° 23′ 59″ E | 0.55 | 0.58 | 1210 | 1062 | 1156 | 148 | 476 | 386 | 3.22 | 1.23 | 2.61 | 11.02 | 14.09 | 15.26 | 1.08 | 20 | E | G, PG |
| Plešné jezero | 48° 46′ 35″ N, 13° 51′ 54″ E | 0.70 | 0.70 | 1342 | 1068 | 1174 | 274 | 1008 | 760 | 3.68 | 1.33 | 2.77 | 104.95 | 53.66 | 60.90 | 1.13 | 25 | NE | G, PG |
| Grosser Arbersee | 49° 05′ 54″ N, 13° 09′ 03″ E | 0.89 | 0.79 | 1292 | 918 | 1062 | 374 | 1212 | 1467 | 3.24 | 0.83 | 3.92 | 332.49 | 154.53 | 171.49 | 1.11 | 22 | E | GN |
| Rachelsee | 48° 58′ 38″ N, 13° 24′ 04″ E | 0.56 | 0.72 | 1263 | 1057 | 1150 | 206 | 809 | 608 | 3.93 | 1.33 | 2.95 | 50.66 | 37.26 | 41.41 | 1.11 | 23 | S | GN |
| Grosser Rachel-Alter See | 48° 58′ 28″ N, 13° 23′ 36″ E | 0.62 | 0.58 | 1437 | 1077 | 1213 | 360 | 820 | 830 | 2.28 | 0.99 | 2.31 | 122.51 | 56.60 | 63.83 | 1.13 | 26 | SE | GN |
| Kleiner Rachel | 48° 59′ 19″ N, 13° 23′ 09″ E | 0.51 | 0.64 | 1281 | 1070 | 1155 | 211 | 982 | 761 | 4.65 | 1.29 | 3.61 | 78.84 | 53.21 | 58.14 | 1.09 | 21 | N | GN |
| Kleiner Arbersee | 49° 07′ 28″ N, 13° 07′ 10″ E | 0.35 | 0.41 | 1268 | 907 | 1059 | 361 | 1798 | 1090 | 4.98 | 1.65 | 3.02 | 353.75 | 148.09 | 162.99 | 1.10 | 22 | N | GN |
| Hirschbach | 49° 02′ 32″ N, 13° 22′ 23″ E | 0.44 | 0.64 | 1237 | 1085 | 1165 | 152 | 407 | 382 | 2.68 | 1.07 | 2.51 | 11.82 | 11.01 | 12.24 | 1.11 | 25 | S | MS |
| Hirschbach II[c] | 49° 01′ 47″ N, 13° 21′ 48″ E | 0.42 | 0.30 | 1061 | 945 | 999 | 116 | 453 | 447 | 3.91 | 1.01 | 3.85 | 11.74 | 16.18 | 17.34 | 1.07 | 19 | SE | GR |
| Schwarzbach[d] | 48° 57′ 17″ N, 13° 32′ 08″ E | 0.56 | 0.72 | 1272 | 1016 | 1107 | 256 | 675 | 718 | 2.64 | 0.94 | 2.80 | 62.04 | 36.83 | 41.36 | 1.12 | 23 | SE | GR |
| Malá Kotelní jáma | 50° 44′ 52″ N, 15° 32′ 03″ E | 0.61 | 0.64 | 1421 | 1097 | 1246 | 324 | 590 | 360 | 1.82 | 1.64 | 1.11 | 34.41 | 18.13 | 21.99 | 1.21 | 32 | SE | PH, GN |
| Velká Kotelní jáma | 50° 45′ 02″ N, 15° 32′ 14″ E | 0.79 | 0.74 | 1406 | 1125 | 1275 | 281 | 502 | 640 | 1.79 | 0.78 | 2.28 | 45.14 | 25.39 | 30.64 | 1.21 | 32 | S | PH, MS, GR |
| Labský důl | 50° 46′ 07″ N, 15° 33′ 07″ E | 0.80 | 0.77 | 1303 | 1018 | 1124 | 285 | 975 | 770 | 3.42 | 1.27 | 2.70 | 106.98 | 62.18 | 74.23 | 1.19 | 27 | SE | GR |
| Harrachova jáma | 50° 45′ 18″ N, 15° 33′ 10″ E | 1.00 | I.21 | 1353 | 1168 | 1270 | 185 | 278 | 555 | 1.50 | 0.50 | 3.00 | 14.27 | 11.84 | 14.42 | 1.22 | 34 | NE | GR |
| Úpská jáma | 50° 43′ 59″ N, 15° 43′ 22″ E | 0.61 | 0.74 | 1498 | 1045 | 1250 | 453 | 782 | 1300 | 1.73 | 0.60 | 2.87 | 230.26 | 86.29 | 101.96 | 1.18 | 30 | E | GR, GD |
| Velká Studniční jáma | 50° 43′ 17″ N, 15° 42′ 46″ E | 0.79 | 0.79 | 1500 | 1114 | 1266 | 386 | 724 | 367 | 1.88 | 1.97 | 0.95 | 51.28 | 21.62 | 25.63 | 1.19 | 30 | S | PH, MS |
| Malá Studniční jáma | 50° 43′ 30″ N, 15° 43′ 01″ E | 0.74 | 0.78 | 1478 | 1222 | 1334 | 256 | 405 | 380 | 1.58 | 1.07 | 1.48 | 19.70 | 12.34 | 14.78 | 1.20 | 32 | SE | PH, MS |
| Mały Śnieżny Kocioł | 50° 46′ 56″ N, 15° 33′ 25″ E | 0.64 | I.15 | 1476 | 1181 | 1306 | 295 | 726 | 440 | 2.46 | 1.65 | 1.49 | 47.12 | 25.77 | 31.04 | 1.20 | 30 | NE | GR |
| Wielki Śnieżny Kocioł | 50° 46′ 47″ N, 15° 33′ 39″ E | 0.83 | 0.85 | 1488 | 1246 | 1330 | 242 | 805 | 526 | 3.33 | 1.53 | 2.17 | 51.24 | 34.88 | 41.99 | 1.20 | 29 | N | GR |
| Czarny Kocioł | 50° 46′ 58″ N, 15° 35′ 08″ E | 0.73 | 0.85 | 1346 | 1117 | 1202 | 229 | 473 | 413 | 2.07 | 1.15 | 1.80 | 22.37 | 14.91 | 17.73 | 1.19 | 30 | N | GR |
| Wielki Staw | 50° 45′ 31″ N, 15° 41′ 33″ E | 0.72 | 0.82 | 1403 | 1200 | 1276 | 203 | 581 | 757 | 2.86 | 0.77 | 3.73 | 44.64 | 36.88 | 41.94 | 1.14 | 23 | NE | GR |
| Mały Staw | 50° 44′ 52″ N, 15° 42′ 05″ E | 0.70 | 0.84 | 1391 | 1108 | 1225 | 283 | 1507 | 934 | 5.33 | 1.61 | 3.30 | 199.17 | 101.84 | 114.62 | 1.13 | 23 | N | GR |
| Łomniczka | 50° 44′ 30″ N, 15° 44′ 02″ E | 0.56 | 0.74 | 1411 | 1051 | 1222 | 360 | 899 | 826 | 2.50 | 1.09 | 2.29 | 133.66 | 63.44 | 74.66 | 1.18 | 30 | NE | GR |
| Velká kotlina | 50° 03′ 18″ N, 17° 14′ 19″ E | 0.82 | 0.83 | 1350 | 1156 | 1258 | 194 | 299 | 405 | 1.54 | 0.74 | 2.09 | 11.75 | 9.79 | 11.86 | 1.21 | 33 | SE | PH |

$E_{max., min., mean}$ — maximal, minimal and mean cirque elevation in m asl.
[a] Lithology: MS — mica schist, PG — paragneis, GD — granodiorite, GR — granite, GN — gneiss, and PH — phyllite.
[b] In the work of Mentlík et al. (2010), this feature is described as "lower cirque."
[c] In the work of Ergenzinger (1967), this feature is described as Wiesriegelkar.
[d] In the work of Ergenzinger (1967), this feature is described as Bärenriegelkar.

within the profile should have ignored the regions of a cirque that were post-glacially altered and minimised the likelihood that nonglacial landforms were described instead of glacial features. Therefore, it is necessary to abstract glacial and postglacial accumulation landforms (e.g., moraines, slope talus, and debris-flows) that could have influenced the shape of the longitudinal profile curve and, consequently, the placement of the headwall foot. This correction could be carried out using an extrapolation of the bedrock line in the foot of the cirque headwall and possibly the cirque bottom.

### 5.2. Informative value of k-curve

In addition to $k$-coefficients, the rate of cirque overdeepening can also be characterised by several morphometric traits. Correlation

**Table 2**
Correlation matrices of morphometric characteristics of the studied cirques; marked correlations (bold) were significant at $p<0.05$ as determined using t-tests (N = 27).

| Variable | *H* | *L* | *W* | *L/H* | *L/W* | *W/H* | *V* | *2D* area | *3D* area | *3D/2D* | Mean gradient |
|---|---|---|---|---|---|---|---|---|---|---|---|
| *H* | 1.00 | **0.51** | **0.61** | −0.20 | 0.15 | −0.28 | **0.69** | **0.60** | **0.62** | 0.27 | 0.27 |
| *L* | **0.51** | 1.00 | **0.69** | **0.70** | **0.44** | 0.33 | **0.85** | **0.89** | **0.89** | **−0.39** | **−0.46** |
| *W* | **0.61** | **0.69** | 1.00 | 0.30 | −0.27 | **0.57** | **0.90** | **0.90** | **0.91** | −0.32 | −0.33 |
| *L/H* | −0.20 | **0.70** | 0.30 | 1.00 | **0.42** | **0.63** | 0.38 | **0.50** | **0.48** | **−0.74** | **−0.82** |
| *L/W* | 0.15 | **0.44** | −0.27 | **0.42** | 1.00 | **−0.40** | 0.05 | 0.07 | 0.07 | −0.04 | −0.14 |
| *W/H* | −0.28 | 0.33 | **0.57** | **0.63** | **−0.40** | 1.00 | 0.36 | **0.46** | **0.44** | **−0.74** | **−0.75** |
| *V* | **0.69** | **0.85** | **0.90** | 0.38 | 0.05 | 0.36 | 1.00 | **0.98** | **0.98** | −0.27 | −0.28 |
| *2D* area | **0.60** | **0.89** | **0.90** | **0.50** | 0.07 | **0.46** | **0.98** | 1.00 | **1.00** | −0.36 | **−0.40** |
| *3D* area | **0.62** | **0.89** | **0.91** | **0.48** | 0.07 | **0.44** | **0.98** | **1.00** | 1.00 | −0.32 | −0.37 |
| *3D/2D* | 0.27 | **−0.39** | −0.32 | **−0.74** | −0.04 | **−0.74** | −0.27 | −0.36 | −0.32 | 1.00 | **0.96** |
| Mean gradient | 0.27 | **−0.46** | −0.33 | **−0.82** | −0.14 | **−0.75** | −0.28 | **−0.40** | −0.37 | **0.96** | 1.00 |

analyses (Table 3) of the studied group of cirques showed that *k*-values correlated with *L/H*, *3D/2D* ratios, and mean cirque gradients; whereas the highest correlation coefficient value (0.73) was observed for the *3D/2D* ratio. The best means of approximating *k*-values using classic morphometric tools is the expression using surface area, cirque planform ratio (*3D/2D*) or mean gradient.

Based on theories of cirque development over time (Gordon, 1977; Olyphant, 1981; Brook et al., 2006; Evans, 2006), we can assume that *k*-values change as a cirque ages. Based on the development of diagrams of long profile time evolution according to Gordon (1977) and later in similar works (Brook et al., 2006; Evans, 2006), *k*-values can be determined using a simple calculation; these diagrams also illustrate that the change in *k*-values over time is linear for cirques in alpine and highland relief environments. The *k*-coefficients appear to be a strong expression of the degree of cirque development.

Differences in both morphometric characteristics (see above) and *k*-values for cirques in the Šumava Mts. and the High Sudetes were also observed. The cirques in the High Sudetes had a greater degree of overdeepening than cirques in the Šumava Mts. A greater extent of overdeepening of cirques in the High Sudetes probably relates to a more extensive and intense glaciation. Deglaciation of the Šumava Mts. (Raab, 1999; Mentlík et al., 2010) occurred much earlier than in the Giant Mts. (Engel et al., 2010).

This difference cannot be explained by differences in lithology because one-way ANOVA did not show (95% significance level) a significant relationship between lithologic type and $k_h$ and $k_s$ values.

### 5.3. Cirque classifications

Previously published cirque classifications have been either only descriptive, by taking into account cirque genesis together with topography or geology (Rudberg, 1954; Trenhaile, 1976; Gordon, 1977; Vilborg, 1977); or as in the case of recent classifications, they have taken into account basic morphometric size and shape characteristics together with the cirque geology or aspect (García-Ruiz et al., 2000; Ruiz-Fernández et al., 2009). García-Ruiz et al. (2000) classified 194 cirques of the central Pyrenees (Spain) into four groups using cluster analysis (minimization of Euclidean distances and selection from the dendrogram) based on certain morphometric characteristics (*L*, *W*, *H*, *A*, *L/W*, and *L/H*). These authors noted that their analyses showed that certain environmental variables (altitude, aspect, and lithology) had a limited influence on both the shape and size variables of those glacial cirques. Discriminant analysis showed

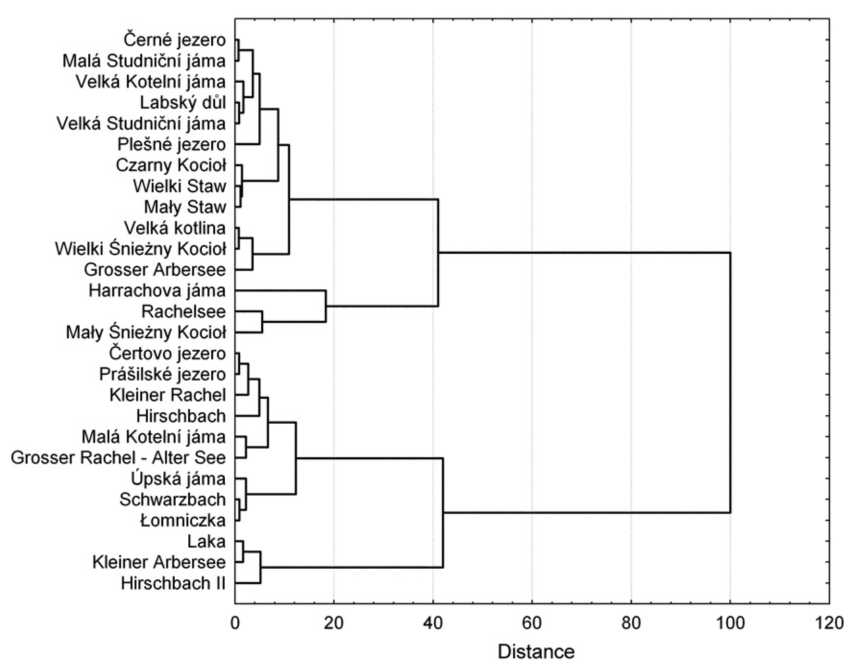


**Fig. 5.** Tree clustering of cirques according to *k*-highest and *k*-steepest (Euclidean distance measures and amalgamation rule by Ward's method).

**Table 3**
Classification matrix for the first group of analyses: randomly chosen cirque for which the discriminant function coefficients were defined, the second cross-validation group and both groups together.

| Class | 1st group analysis (%) | Cross-validation (%) | Both (%) |
|---|---|---|---|
| X | 88.89 | 83.33 | 86.67 |
| Y | 100.00 | 57.14 | 75.00 |
| Total | 92.86 | 69.23 | 81.48 |

that altitude, aspect, and lithology explained the classification of only ~66% of the Pyrenean cirques. The other discriminating factors were ascribed to the influence of the presence of faults, the resistance of rocks and preglacial relief. Studies of cirque morphometry from different parts of the world (Aniya and Welch, 1981; Evans and Cox, 1995; García-Ruiz et al., 2000; Federici and Spagnolo, 2004; Hughes et al., 2007; Ruiz-Fernández et al., 2009) have shown that the influence of all the above-mentioned factors on the size and shape of cirques cannot be generalised.

According to the successful classification performed using GDA (Table 3), the existence of a close relationship between the degree of overdeepening and morphometric characteristics was detected for the group of Bohemian Massif cirques studied here. Cirque classifications based on *k*-values coincided with morphometric-based classifications in 81% of the cases. In other words, the classification of cirques based on a genetic perspective (*k*-curve as defined by Haynes, 1968) is compatible with classification methods based on cirque morphology (morphological indices in accordance with Evans and Cox, 1995). Therefore, this study demonstrated that the classification of cirques according to the degree of overdeepening corresponded more closely with cirque morphometry than with environmental variables, as shown by García-Ruiz et al. (2000) and Ruiz-Fernández et al. (2009).

**Table 4**
Posterior probabilities of classifications; incorrect classifications are marked with *; cirques from the first group of analyses (which defined the discriminant function coefficients) are marked with a ***bold italic*** font; observed classifications were based on $k_h$ and $k_s$ in two classes *X* and *Y*.

| Cirque name | Observed class | X | Y |
|---|---|---|---|
| ***Černé jezero*** | X | 0.88 | 0.12 |
| Čertovo jezero | Y | 0.10 | 0.90 |
| ***Laka*** | Y | 0.14 | 0.86 |
| ***Prášilské jezero*** | Y | 0.32 | 0.68 |
| ***Plešné jezero*** | X | 0.81 | 0.19 |
| ***Velká kotlina*** | X | 0.85 | 0.15 |
| Malá Kotelní jáma* | Y | 1.00 | 0.00 |
| Velká Kotelní jáma | X | 0.84 | 0.16 |
| ***Labský důl*** | X | 0.97 | 0.03 |
| Harrachova jáma | X | 0.71 | 0.29 |
| ***Úpská jáma**** | Y | 0.42 | 0.58 |
| Velká Studniční jáma | X | 1.00 | 0.00 |
| Malá Studniční jáma | X | 0.93 | 0.07 |
| ***Grosser Arbersee**** | X | 0.13 | 0.87 |
| ***Rachelsee*** | X | 0.66 | 0.34 |
| ***Grosser Rachel-Alter See*** | Y | 0.38 | 0.62 |
| Kleiner Rachel | Y | 0.44 | 0.56 |
| Kleiner Arbersee* | Y | 0.82 | 0.18 |
| Hirschbach | Y | 0.39 | 0.61 |
| Hirschbach II | Y | 0.10 | 0.90 |
| ***Schwarzbach*** | Y | 0.32 | 0.68 |
| ***Mały Śnieżny Kocioł*** | X | 1.00 | 0.00 |
| Wielki Śnieżny Kocioł | X | 0.99 | 0.01 |
| ***Czarny Kocioł*** | X | 0.94 | 0.06 |
| Wielki Staw* | X | 0.28 | 0.72 |
| ***Mały Staw*** | X | 0.92 | 0.08 |
| Łomniczka* | Y | 0.86 | 0.14 |

Divergences in cirque classifications, or incorrect categorization into groups, can be explained in several ways: (i) Although it emerged that *k*-curves are related (a significant correlation existed) to some morphometric characteristics [$k_h$ vs. *L*/*H* (−0.50), *3D*/*2D* (0.70), mean gradient (0.62); $k_s$ vs. *L*/*H* (−0.42), *3D*/*2D* (0.65), mean gradient (0.61)], *k*-curves provide different information and cannot be replaced entirely by morphometric methods. In other words, a difference exists between strictly morphological characteristics (sensu Evans and Cox, 1995) and genetic aspects of cirques that are represented by *k*-curves (sensu Haynes, 1968). (ii) The set of standard morphometric characteristics does not have to be complete, or other independent sizes or indices that could better characterise a cirque from a genetic perspective can be missing. (iii) If the set of studied cirques with an analogous genesis was larger, the influence of abnormally-developed cirques would be statistically low. A better determination of cirque groups could be obtained by addressing these factors.

## 6. Conclusions

Mathematical analyses were used to demonstrate the potential benefits and limitations of using *k*-curves in real scenarios:

(i) It is necessary to correctly and unequivocally identify the longitudinal profile and input variables (position of the crest and cirque headwall or the deepest point of the cirque) to obtain a correct definition of the *k*-value. The *k*-values cannot be negative. The ratio between the height of the headwall and cirque floor deepening is constant and does not depend on the value of the *k*-coefficient.

(ii) Knowledge of the cirque headwall height allows for the mathematical calculation (theoretical) of cirque overdeepening (i.e., the maximum depth of the cirque floor). If the *k*-curve could be considered as approximation to the longitudinal profile of cirque, then it is possible according to the *k*-curve equation to calculate hypothetical cirque depth and thus thickness of sedimentary fill of the cirque bottom or depth of the lake.

(iii) According to the cirque development diagram for long profile time evolution (sensu Brook et al., 2006), we can show that changes in *k*-values are linear over time.

(iv) Classification of cirques according to *k*-values corresponded to the classifications based on morphometric characteristics represented by their basis (*L*/*W*, *H*, and *3D*/*2D*). Furthermore, results of these classifications corresponded to regional divisions and reflected the different intensities and development of mountain glaciation in the northeastern (the High Sudetes) and southwestern parts (the Šumava Mts.) of the Bohemian Massif. Cirques of the High Sudetes (northeastern part of the Bohemian Massif) had a higher degree of overdeepening than cirques of the Šumava Mts.; and the High Sudetes cirques were deeper, shorter, and narrower. A higher rate of overdeepening (greater *k*-value) of cirques in the High Sudetes was caused by longer-lasting glaciation.

## Acknowledgements

This study was funded by the Grant Agency of the Czech Republic (P209/10/0519) and the project of the Czech Ministry of Education, Youth and Sports (MSM 0021620831). The authors would like to acknowledge Krkonoše N.P., Šumava N.P. and Jeseníky PLA administrations for granting permission to work in the region.

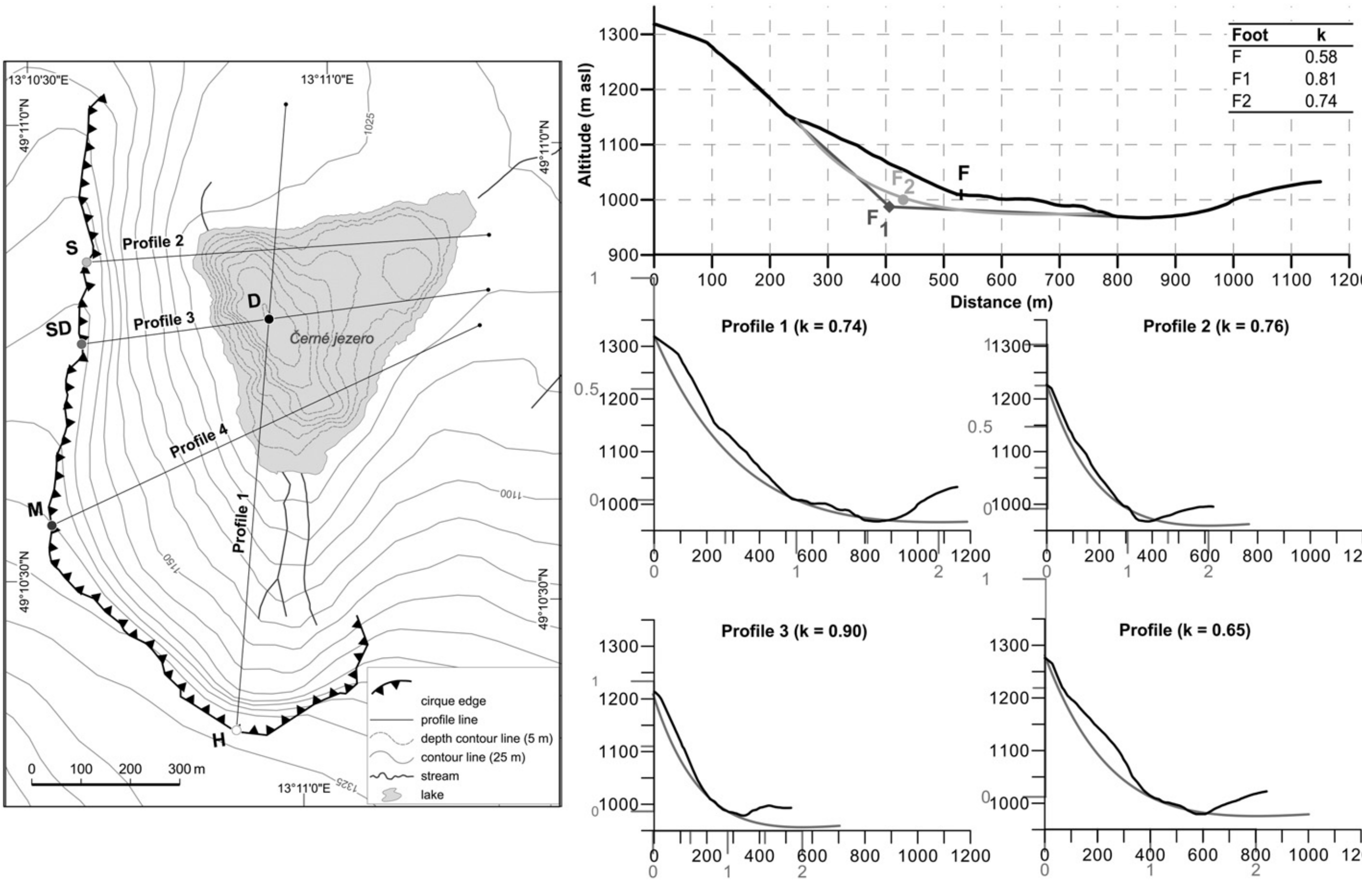


**Fig. 6.** Visualisation of the dependence of *k*-values on the profile location within the cirque and on the location of the headwall foot for the Černé jezero cirque (the Bohemian Forest). S — the point above the steepest part of the cirque; SD — the point above the steep part of the headwall and the deepest point of the cirque; M — midpoint of the cirque crest; H — the highest altitude of the cirque crest. The grey scale in profiles 1–4 indicates the *k*-curve *x* and *y* values.

## References


Aniya, M., Welch, R., 1981. Morphometric analysis of Antarctic cirques from photogrammetric measurements. Geografiska Annaler Series A, Physical Geography 63 (1/2), 41–53.

Babůrek, J., Pertoldová, J., Verner, K., Jiřička, J., 2006. Průvodce geologií Šumavy. Správa NP a CHKO Šumava a Ceská Geologická Služba, Praha, Vimperk, Czech Republic. 128 pp.

Bayberger, F., 1886. Geographisch-geologische Studien aus dem Böhmerwalde. Die die Spuren alter Gletscher, die Seen und die Täler des Böhmerwaldes. Petermanns Geographische Mitteilungen 81, 1–63.

Benn, D.I., Evans, D.J.A., 2010. Glaciers and Glaciation. Arnold, London, pp. 311–312.

Bennett, M.R., Glasser, N.F., 2009. Glacial geology. Ice Sheets and Landforms. Wiley-Blackwell, Chichester, UK. 385 pp.

Brook, M.S., Kirkbride, M.P., Brock, B.W., 2006. Cirque development in a steadily uplifting range: rates of erosion and long-term morphometric change in alpine cirques in the Ben Ohau Range, New Zealand. Earth Surface Processes and Landforms 31, 1167–1175.

Chlupáč, I., Brzobohatý, R., Kovanda, J., Stráník, Z., 2002. Geologická minulost České republiky. Academia, Praha, Czech Republic. 436 pp.

Chmal, H., Traczyk, A., 1999. Die Vergletscherung des Riesengebirges. Zeitschrift für Geomorphologie N.F., Supplement-Band 113, 11–17.

Czudek, T., 2005. Vývoj reliéfu krajiny České republiky v kvartéru. Moravské Zemské Muzeum, Brno, Czech Republic. 238 pp.

Davis, P.T., 1999. Cirques of the Presidential Range, New Hampshire, and surrounding alpine areas in the northeastern United States. Géographie Physique et Quaternaire 53 (1), 25–45.

Engel, Z., 2007. Late Pleistocene glaciation in the Krkonoše Mts. In: Goudie, A.S., Kalvoda, J. (Eds.), Geomorphological Variations. P3K, Praha, Czech Republic, pp. 269–285.

Engel, Z., Nývlt, D., Křížek, M., Treml, V., Jankovská, V., Lisá, L., 2010. Sedimentary evidence of landscape and climate history since the end of MIS 3 in the Krkonoše Mountains, Czech Republic. Quaternary Science Reviews 29, 913–927.

Ergenzinger, P., 1967. Die eiszeitliche Vergletscherung des Bayerischen Waldes. Eiszeitalter und Gegenwart 18, 152–168.

Evans, I.S., 1977. World-wide variations in direction and concentration of cirque and glaciation aspect. Geografiska Annaler 59A (3/4), 151–175.

Evans, I.S., 2006. Allometric development of glacial cirque form: geological, relief and regional effects on the cirques of Wales. Geomorphology 80, 245–266.

Evans, I.S., Cox, N.J., 1995. The forms of glacial cirques in the English Lake District, Cumbria. Zeitschrift für Geomorphologie N.F. 39 (2), 175–202.

Federici, P.R., Spagnolo, M., 2004. Morphometric analysis on the size, shape and areal distribution of glacial cirques in the Maritime Alps (western French-Italian Alps). Geografiska Annaler Series A, Physical Geography 86 (3), 235–248.

García-Ruiz, J.M., Gómez-Villar, A., Ortigosa, L., Martí-Bono, C., 2000. Morphometry of glacial cirques in the central Spanish Pyrenees. Geografiska Annaler Series A, Physical Geography 82 (4), 433–442.

Gordon, J.E., 1977. Morphometry of cirques in the Kintail-Affric-Cannich area of northwest Scotland. Geografiska Annaler Series A, Physical Geography 59 (3/4), 177–194.

Graf, W.L., 1976. Cirques as glacier locations. Arctic and Alpine Research 8 (1), 79–90.

Hall, A.M., Migoń, P., 2010. The first stages of erosion by ice sheets: evidence from central Europe. Geomorphology 123, 349–363.

Hauner, U., 1980. Untersuchungen zur klimagesteuerten tertiären und quartären Morphogenese des Inneren Bayerischen Waldes (Rachel-Lusen) unter besonderer Berücksichtigung pleistozän kaltzeitlicher Formen und Ablagerungen. Regensburger Geographische Schriften 14, 1–198.

Haynes, V.M., 1968. The influence of glacial erosion and rock structure on corries in Scotland. Geografiska Annaler 50 A (4), 221–234.

Haynes, V.M., 1998. The morphological development of alpine valley heads in the Antarctic peninsula. Earth Surface Processes and Landforms 23, 53–67.

Huberty, C.J., 1994. Applied discriminant analysis. Wiley, New York. 466 pp.

Hughes, P.D., Gibbard, J.C., Woodward, J.C., 2007. Geological controls on Pleistocene glaciation and cirque form in Greece. Geomorphology 88, 242–253.

Isarin, R.F.B., Renssen, H., Koster, E.A., 1997. Surface wind climate during the Younger Dryas in Europe as inferred from aeolian records and model simulations. Palaeogeography, Palaeoclimatology, Palaeoecology 134, 127–148.

Jeník, J., 1961. Alpinská vegetace Krkonoš, Králického Sněžníku a Hrubého Jeseníku: teorie anemo-orografických systémů. Nakl. ČSAV, Praha, Czech Republic. 409 pp.

Králík, F., Sekyra, J., 1969. Geomorfologický přehled Krkonoš. In: Fanta, J. (Ed.), Příroda Krkonošského Národního Parku. SZN, Praha, Czech Republic, pp. 59–87.

Kunský, J., 1948. Geomorfologický náčrt Krkonoš. In: Klika, J. (Ed.), Příroda v Krkonoších. Česká Grafická Unie, Praha, Czech Republic, pp. 54–89.

Manly, B.F.J., 2005. Multivariate Statistical Methods. Chapman and Hall/CRC, Boca Raton, FL. 214 pp.

Martini, I.P., Brookfield, M.E., Sadura, S., 2001. Principles of Glacial Geomorphology and Geology. Prentice Hall Inc., Upper Saddle River, NJ. 381 pp.

Meloun, M., Militký, J., Hill, M., 2005. Počítačová analýza vícerozměrných dat v příkladech. Academia, Praha, Czech Republic. 449 pp.

Mentlík, P., Minár, J., Břízová, E., Lisá, L., Tábořík, P., Stacke, V., 2010. Glaciation in the surroundings of Prášilské Lake (Bohemian Forest, Czech Republic). Geomorphology 117, 181–194.
Mercier, J.-L., Bourlès, D.L., Kalvoda, J., Engel, Z., Braucher, R., 2000. Preliminary results of $^{10}$Be dating of glacial landscape in the Giant Mountains. Acta Universitatis Carolinae, Geographica 35 (Suppl. 2000), 157–170.
Meyer, H.-H., Kottmeier, Ch., 1989. Die atmosphärische Zirkulation in Europa im Hochglazial der Weichsel-Eiszeit — abgeleitet von Paläowind-Indikatoren und Modellsimulationen. Eiszeitalter und Gegenwart 39 (1), 10–18.
Migoń, P., 1999. The role of preglacial relief in the development of mountain glaciation in the Sudetes, with the special references to the Karkonosze Mountains. Zeitschrift für Geomorphologie N.F., Supplement-Band 113, 33–44.
Olyphant, G.A., 1981. Allometry and cirque evolution. Geological Society of America Bulletin, Part I 92, 679–685.
Partsch, J., 1894. Die Vergletscherung des Riesengebirges zur Eiszeit. Forsch. z. Deutsch. Landes und Folkskunde 8 (2), 103–194.
Priehäusser, G., 1930. Die Eiszeit im Bayerischen Wald. Abhandlungen der Geologischen Landesuntersuchung des bayerischen Oberbergamtes Munchen, Heft, 2, pp. 5–47.
Prosová, M., 1958. Kvartér Hrubého Jeseníku: vrcholná část hlavního hřbetu. 125 s. Ph.D. Dissertation, Univerzita Karlova, Praha.
Prosová, M., Sekyra, J., 1961. Vliv severovýchodní exposice na vývoj reliéfu v pleistocénu. Časopis pro Mineralogii a Geologii VI (4), 448–463.
Raab, T., 1999. Würmzeitliche Vergletscherung des Bayerischen Waldes im Arbergebiet. Regensburger Geographische Schriften 32, 1–327.
Raab, T., Völkel, J., 2003. Late Pleistocene glaciation of the Kleiner Arbersee area in the Bavarian Forest, south Germany. Quaternary Science Reviews 22, 581–593.
Rasemann, S., Schmidt, J., Schrott, L., Dikau, R., 2004. Geomorphometry in mountain terrain. In: Bishop, M., Shroder Jr., J. (Eds.), Geographic Information Science and Mountain Geomorphology. Springer-Praxis Books in Geophysical Sciences, Berlin, pp. 101–146.
Rathsburg, A., 1928. Die Gletscher des Böhmerwaldes zur Eiszeit. Bericht der Naturwissenschaftlichen Gesellschaft zu Chemnitz 22, 65–161.
Reuther, A.U., 2007. Surface exposure dating of glacial deposits from the last glacial cycle. Evidence from the eastern Alps, the Bavarian Forest, the southern Carpathians and the Altai Mountains. Relief Boden Palaeoklima 21, 1–213.
Rudberg, S., 1954. Västerbottens berggrundsmorfologi. Ett försök till rekonstruktion av preglaciala erosionsgenerationer i Sverige (English summary) Geographica 25, 1–457.
Ruiz-Fernández, J., Poblete-Piedrabuena, M.A., Serrano-Muela, M.P., Martí-Bono, C., García-Ruiz, J.M., 2009. Morphometry of glacial cirques in the Cantabrian Range (northwest Spain). Zeitschrift für Geomorphologie N.F. 53 (1), 47–68.
StatSoft, Inc., 2009. STATISTICA (data analysis software system), version 9.0. www.statsoft.com.
Traczyk, A., 1989. Zlodowacenie doliny Łomnicy w Karkonoszach oraz poglady na ilość zlodowaceń plejstoceńskich w średnich górach Europy. Czasopismo Geograficzne 60 (3), 267–286.
Trenhaile, A.S., 1976. Cirque morphometry in the Canadian Cordillera. Annals of the Association of American Geographers 66 (3), 451–462.
Vilborg, L., 1977. The cirque forms of Swedish Lapland. Geografiska Annaler Series A, Physical Geography 59 (3/4), 89–150.
Vitásek, F., 1924. Naše hory ve věku ledovém. Sborník Československé společnosti zeměpisné 1924, XXX, pp. 85–105.
Vočadlová, K., Křížek, M., 2005. Glacial landforms in the Černé jezero Lake area. Miscellanea Geographica Universitatis Bohemiae Occidentalis, 11, pp. 47–63.
Vočadlová, K., Křížek, M., 2009. Comparison of glacial relief landforms and the factors which determine glaciation in the surroundings of Černé jezero Lake and Čertovo jezero Lake (Šumava Mts., Czech Republic). Moravian Geographical Reports 17 (2), 2–14.
Vočadlová, K., Křížek, M., Čtvrtlíková, M., Hekera, P., 2007. Hypothesis for the last stage of glaciation in the Černé Lake area (Bohemian Forest, Czech Republic). Silva Gabreta 13 (3), 205–216.
Votýpka, J., 1979. Geomorfologie granitového masívu Plechého. Acta Universitatis Carolinae-Geographica XVI (2), 55–83.